

# Gain-Switched Semiconductor Laser Amplifier as an Ultrafast Dynamical Optical Gate

E. Schöll

Institut für Theoretische Physik der RWTH Aachen, D-5100 Aachen, Fed. Rep. Germany

K. Ketterer, E. H. Böttcher, and D. Bimberg

Institut für Festkörperphysik der TU Berlin, Hardenbergstrasse 36, D-1000 Berlin 12

Received 30 November 1987/Accepted 7 January 1988

**Abstract.** A gain-switched semiconductor laser is shown to act as an optical gate with picosecond resolution and amplification for light pulses from another laser source. The amplification mechanism and the gate width change qualitatively when the gate laser undergoes a transition from a pumping rate slightly below the dynamic laser threshold to slightly above the dynamic threshold. If the gate laser is pumped below but close to its dynamical threshold, unsaturated amplification of an external signal pulse occurs over a delay time range between the external optical pulse and the electrical driving pulse of about 100–200 ps which is equivalent to the optical gate width. The signal amplification is observed to increase by two orders of magnitude and the gate width decreases by one order of magnitude if the gate laser is pumped slightly above the dynamical threshold. Amplification then occurs for input signals injected much earlier. A detailed theory of coherent, time-dependent amplification including the nonlinear dynamics of the semiconductor laser is shown to account for the observations. Both amplification regimes, below and above threshold, are reproduced in the numerical simulations. The extremely short and highly sensitive gate range above threshold is identified as being due to the gain maximum related with the first relaxation oscillation of the laser.

**PACS:** 42.55.Px, 42.60.Da, 85.60.Jb

Semiconductor laser amplifiers (SLAs) have recently attracted considerable interest due to their potential application in future optical communication systems [1, 2], in particular as all-optical repeaters. While the basic properties of dc driven SLAs have been studied in detail during the last decade [3–6] theoretical and experimental work on SLAs under time-dependent conditions is rather scarce [7–10]. Under dc injection the laser diode usually operates below threshold and acts as a linear optical amplifier for the incident coherent lightwaves. If the SLA is driven by short current pulses a time varying signal gain results making such a device suitable for fast switching and modulation applications [7, 8, 11].

Recently, some of us have demonstrated for the first time that a conventional Fabry-Perot type SLA

excited by short current pulses acts as an ultrafast optical gate for external optical signals [11]. We observed the time averaged output power emitted by the SLA driven beyond its dynamical threshold to increase strongly if the optical input pulse enters the SLA within a certain time interval. Based on this finding, an all-optical boxcar with a time resolution better than 10 ps was developed.

It is the purpose of the present paper to present additional and decisive experimental results together with a theoretical simulation of the gate effect in order to demonstrate that coherent amplification accounts for our observations. Section 1 summarizes the experimental results on the dynamics of gain-switched SLAs. The dependence of the optical gate effect and its temporal resolution on the electrical driving con-

ditions of the SLA and on the intensity of the input signal is studied in detail. Two completely different “gate regimes” are observed for the SLA slightly below and above threshold, respectively. The basic concept of a dynamic theory of SLAs which was developed recently by one of us [12] is outlined in Sect. 2. Coherent, time-dependent amplification of an incident optical pulse as well as the nonlinear dynamics of the semiconductor laser are taken into account. In contrast to previous treatments of the dynamics of SLAs [10], this theory is not restricted to optical input signals of a duration shorter than the cavity transit time. Furthermore, its application is not limited to weak [10] or strong [9] input signals causing negligible reduction of the gain or gain depletion, respectively, but it takes explicitly into account the interaction of the time varying optical input signal and the time varying gain of the SLA. Therefore, this new concept has a much wider range of validity than previous simple dynamic models of SLAs [8–10] applying only to limiting cases that are seldom met under practical operating conditions. One important new prediction of this theory is that indeed a dramatic optical pulse shortening can be obtained if the time delay between the incident optical pulse and the injection current pulse which drives the SLA is adjusted appropriately. In Sect. 3 the results of the numerical simulations are presented and compared to the experimental results of Sect. 1, and the physical mechanism which leads to the observed dependence of the integral optical output intensity upon the delay time under different operating conditions is explained in terms of the dynamic theory.

### 1. Experimental: Amplification Below and Above Threshold

In order to study the temporal behaviour of dynamic Fabry-Perot semiconductor laser amplifiers the experimental setup shown in Fig. 1 is used. The transient optical input signal for the laser amplifier (ld2) is generated by a gain-switched GaAs/AlGaAs multiple quantum well laser (ld1) [13]. As laser amplifier (ld2) an AlGaAs twin-channel-substrate-mesa-guide laser [14] is utilized. Both laser diodes are excited by avalanche generators (ag1 and ag2). They provide voltage pulses of 40 V (at 50  $\Omega$  load). The voltage pulses have a full width at half maximum (FWHM) of 240 ps. The electrical excitation level of the laser diodes is adjusted by microwave attenuators. The avalanche generators are driven by a common pulse generator running at a repetition rate of 100 kHz. A variable electronic delay unit driven by a sawtooth voltage is used to shift the delay time between the injection

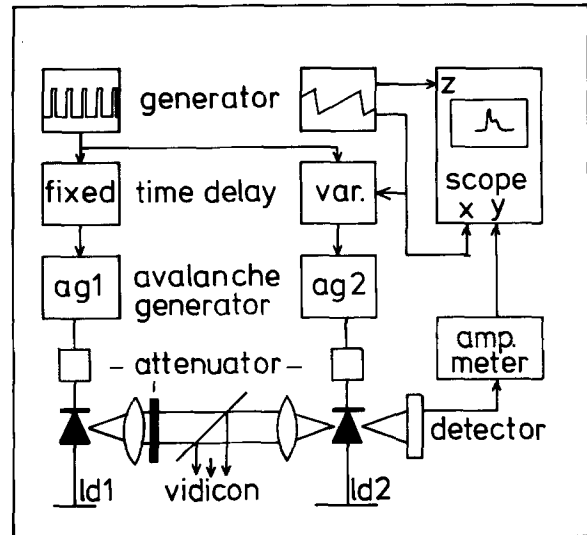


Fig. 1. Schematic of the experimental setup

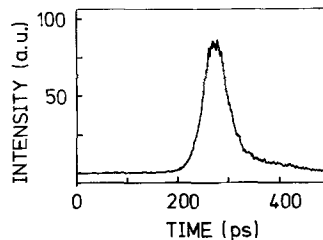


Fig. 2. Synchroscan streak camera record of the optical input signal emitted by ld1

current pulses of ld1 and ld2. The light pulses emitted by ld1 are focused on the active area of the laser amplifier. The light intensity can be varied by means of neutral density filters. A slow integrating Si photodiode monitors the time averaged intensity of the output signal emitted from the rear mirror of ld2. The resulting photocurrent is recorded by a picoammeter and displayed versus the delay time on an x–y real time oscilloscope. The z signal of the oscilloscope blanks out the return motion of the sawtooth voltage. Figure 2 shows a synchroscan streak camera record of the optical pulse emitted by ld1 when ld1 is driven by an injection current pulse such that exactly one relaxation oscillation is emitted. The FWHM of the optical pulse is approximately 56 ps. The measured width in such a synchroscan experiment is not dominated by the width of a single pulse, which is here of the order of 15–20 ps [13], but by the turn-on delay time jitter [15]. The SLA ld2 is driven by an injection current pulse of 160 ps FWHM.

Typical experimental results are shown in Fig. 3. The integrated output intensity  $\int I_{\text{out}}(t)dt$  is plotted versus the delay time  $\tau_d$ . The optical input signal from ld1 is the pulse shown in Fig. 2. The relative maximum

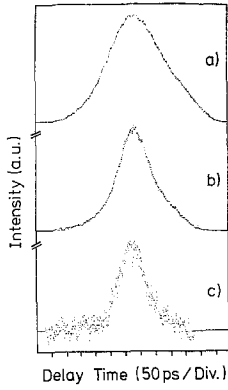


Fig. 3. Integrated output intensity  $\int I_{\text{out}}(t)dt$  plotted versus time delay  $\tau_d$  in relative divisions of 50 ps for ld2 running just below the dynamic threshold and the optical input signal shown in Fig. 2. The attenuation factor of the input light intensity between *a* and *b*, and between *b* and *c* is about 20

$J_0/J_t$  of the current pulse driving the SLA is chosen such that without an optical input signal from ld1 no laser light is emitted by ld2.  $J_t$  is the cw threshold current density of ld2. This corresponds to electrical excitation conditions just below the dynamic “effective threshold” for the emission of laser pulses (relaxation oscillations). Note that this dynamic threshold of  $J_0/J_t$  is pulse shape dependent, and is much higher than the cw threshold  $J_0/J_t=1$  [13,16]. The three curves in Fig. 3 correspond to different optical input signal levels impinging on the laser amplifier. The attenuation factor of the light intensity between (a) and (b), and between (b) and (c) is about 20. The curves are scaled to equal maximum values. The absolute maxima decrease from (a) to (c). The FWHM as well as the signal-to-noise ratio of the integral output intensity decreases with decreasing input light intensity. The delay time between the electrical excitation pulses of ld2 and ld1 is defined in such a way that the larger values of  $\tau_d$  correspond to earlier excitation pulses of ld1. The relative delay time is equivalent to the time difference between the electrical pulse of ld2 and the optical pulse emitted from ld1 onto ld2, since the zero of the  $\tau_d$  axis may be shifted arbitrarily.

If the laser amplifier is excited just above the dynamic effective laser threshold an additional peak appears in a range of delay times corresponding to earlier optical input signals, as shown in Fig. 4a. The amplitudes of the two peaks in Fig. 4a reveal a different dependence on the input light intensity, as shown in Fig. 4a–c. Between curves (a) and (b), and between (b) and (c) the input light intensity is attenuated by a factor of 20 and 50, respectively. The intensities are again scaled to equal maximum values, and the absolute values decrease from (a) to (c). It is obvious from Fig. 4 that the contribution of the correlation signal which is already observed when ld2 is below its dynamic

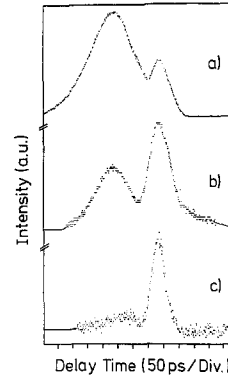


Fig. 4. *a* Same as Fig. 3a, but ld2 is driven just above dynamical threshold. *b* Optical input signal attenuated by about a factor of 20 relative to *a*. *c* Optical input signal attenuated by about a factor of 1000 relative to *a*

threshold, i.e. the peak on the left-hand side, decreases much more rapidly than the peak on the right-hand side if the input intensity is reduced. At sufficiently low input intensities, the lhs peak can be almost neglected as compared to the rhs peak (Fig. 4c). A second important difference between the two peaks is the magnitude of the FWHM. The FWHM of the rhs peak is significantly smaller. The shape of this peak precisely reproduces the shape of the input pulse from ld1 as measured by the synchroscan camera.

## 2. Outline of the Theory of Coherent Dynamical Amplification

First we briefly outline the fundamentals of a theory of coherent dynamical amplification [12]. The incident signal wave must be treated coherently to account properly for interference effects during its transmission through the laser amplifier, and its reflection at the two facets. The signal wave is thus described by space- and time-dependent electric field amplitudes  $E^+(z,t)$  and  $E^-(z,t)$  travelling in the positive (forward) and the negative (backward)  $z$  direction of the SLA resonator, respectively<sup>1</sup>. All the remaining laser modes, excluding the signal mode, may be treated incoherently and described by an axially averaged photon density  $N(t)$ . This is a reasonable approximation for facet reflectivities larger than 20% [17].

The dynamic equations for the signal fields  $E^+$  and  $E^-$  are given by

$$\frac{\partial E^\pm}{\partial t} \pm v_g \frac{\partial E^\pm}{\partial z} = \frac{1}{2}(\Gamma g(n) - \alpha)E^\pm - ikv_g E^\pm, \quad (1)$$

<sup>1</sup> Throughout this paper all fields will be normalized to the dimension of  $(\text{length})^{-3/2}$ , such that the square of the modulus of the electric field strength is equal to the corresponding photon density

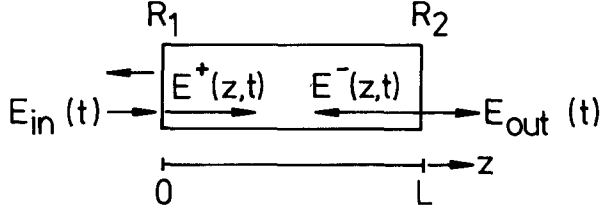


Fig. 5. Schematic representation of the signal field amplitudes in the laser amplifier.  $R_1$  and  $R_2$  are the reflectivities of the facets

where  $v_g \equiv c/n_g$  is the group velocity ( $c$  is the vacuum velocity of light),  $\Gamma$  is the optical confinement factor,  $g(n)$  is the modal gain function depending on the carrier density  $n$ ,  $\alpha$  is the optical loss constant for absorption and scattering in the active and in the cladding region, and  $k$  is the wavevector of the signal in the cavity. The left-hand side of (1) is the total time derivative of  $E^\pm$  as seen by an observer moving with the travelling wave [5], and the factor 1/2 on the right-hand side of (1) results from the fact that the net gain of the field amplitude rather than the intensity is needed here [4, 5]. Equation (1) has to be supplemented by boundary conditions for the crystal facets at  $z=0$  and  $z=L$

$$E^+(0, t) = t_1 E_{in}(t) + r_1 E^-(0, t), \quad (2a)$$

$$E^-(L, t) = r_2 E^+(L, t), \quad (2b)$$

$$E_{out}(t) = t_2 E^+(L, t). \quad (2c)$$

Here  $t_1, t_2$  and  $r_1, r_2$  are the amplitude transmission and reflection coefficients of the two facets, respectively; they are related to the reflectivities  $R_1, R_2$  by

$$\begin{aligned} R_1 &= r_1^2 = 1 - t_1^2, \\ R_2 &= r_2^2 = 1 - t_2^2. \end{aligned} \quad (3)$$

$E_{in}(t)$  and  $E_{out}(t)$  are the incident and the outgoing signal field amplitudes at the facets. The underlying geometrical configuration is represented schematically in Fig. 5.

The main assumption of our theory is that the electron concentration  $n(t)$  is approximated in (1) by a constant during a single-pass transit time of the signal, which is 4 ps for the SLA used (cavity length  $L=300 \mu\text{m}$ , optical group index  $n_g=4$ ). This approximation is well justified since the time-scale over which  $n$  varies appreciably is generally slower than that of the photons; it is of the order of ns, the spontaneous recombination time, as long as we are close to or below threshold. Note, however, that  $n(t)$  may, and in fact does, change from one single-pass to the next.

In this approximation, we can integrate (1) from  $z=0$  to  $z=L$  for the forward or the backward propagating signal wave. The result yields the single-pass

intensity gain

$$\begin{aligned} G_s &\equiv |E^+(L, t)/E^+(0, t-\tau)|^2 \\ &= |E^-(0, t)/E^-(L, t-\tau)|^2 \end{aligned}$$

to be

$$G_s = \exp\{[\Gamma g(n(t)) - \alpha]\tau\}, \quad (4)$$

where  $\tau = L/v_g$  is the single-pass transit time. The total outgoing signal amplitude  $E_{out}(t)$  is obtained by summing over all forward and backward propagating waves with appropriate time delays and phase factors using the boundary conditions (2)

$$\begin{aligned} E_{out}(t) &= (1 - R_1)^{1/2} (1 - R_2)^{1/2} \exp(-ikL) \\ &\times \left\{ \sum_{m=0}^{\infty} E_{in}[t - (2m+1)\tau] (R_1 R_2)^{m/2} \right. \\ &\times \left. \prod_{l=0}^{2m} [G_s(t - l\tau)]^{1/2} \exp(-2mikL) \right\}. \end{aligned} \quad (5)$$

The corresponding normalized output intensity is

$$|E_{out}(t)|^2 = (1 - R_1)(1 - R_2) G_s(t) \Sigma(t), \quad (6)$$

where the memory function  $\Sigma(t)$  contains all the delay and interference terms. The field distributions  $E^\pm(z, t)$  inside the cavity can be computed by integrating (1) from  $z$  to  $L$  using the boundary conditions (2b, c) and (5) [12].

The nonlinear dynamics of the carrier density  $n$  and of the photon density  $N$  in the cavity modes excluding the signal mode are described by rate equations [12, 16–18]

$$dn/dt = \eta J(t)/(ed) - R_{sp}(n) - g(n)(N + \bar{S}), \quad (7)$$

$$dN/dt = [\Gamma g(n) - \kappa]N + \beta R_{sp}(n), \quad (8)$$

where  $J(t)$  is the externally given time varying injection current density of  $\text{ld}2$ ,  $\eta$  is the electron injection efficiency,  $d$  is the thickness of the active layer,  $R_{sp}(n)$  is the spontaneous recombination rate,  $\kappa$  is the total inverse photon lifetime including absorption, scattering, and mirror losses of the cavity modes, and  $\beta$  is the spontaneous emission factor into the laser modes. The coupling with the coherent signal wave occurs through the last term in (7) which represents the recombination rate due to stimulated emission into the signal mode. Here  $\bar{S}$  is the axially averaged photon density corresponding to the travelling signal wave

$$\begin{aligned} \bar{S}(t) &= L^{-1} \int_0^L [|E^+(z, t - (L-z)v_g^{-1})|^2 \\ &+ |E^-(z, t + (L-z)v_g^{-1})|^2] dz. \end{aligned} \quad (9)$$

It is given explicitly by [12]

$$\begin{aligned} \bar{S}(t) &= [G_s(t) - 1] [1 + R_2 G_s(t)] \\ &\times (1 - R_1) \Sigma(t) / \ln G_s(t). \end{aligned} \quad (10)$$

Equations (7, 8, 10) constitute a complicated system of delay differential equations due to the occurrence of the delayed carrier densities  $n(t-\tau)$ ,  $n(t-2\tau)$ ,  $n(t-3\tau)$ , ... in (10). They can be integrated numerically for given injection current pulses  $J(t)$  and incident signals  $E_{\text{in}}(t)$ . The result gives the electron density  $n$ , the amplified spontaneous emission  $N$ , the output signal  $|E_{\text{out}}|^2$ , and the single-pass gain  $G_s$  as a function of time.

In the special case of a time independent input signal  $E_{\text{in}}$  and time independent injection current  $J$ , the stationary solutions of (7, 8, 10) reduce to the familiar result of an active Fabry-Perot cavity [4] with a static single-pass gain  $G_s$ .

A different theoretical approach was taken by Ikeda [8], and Mukai et al. [2, 3] who considered *incoherent* optical amplification. In order to compare our results with their model, we introduce the total photon density

$$S \equiv N + \bar{S} \quad (11)$$

which includes both the amplified spontaneous emission and the amplified signal. Incoherent optical amplification is then described [2, 3, 8] by

$$dS/dt = [\Gamma g(n) - \kappa]S + \beta R_{sp}(n) + P_{\text{in}}(t) \quad (12)$$

where  $P_{\text{in}}(t)$  is the given optical pumping rate, i.e., the number of injected photons per unit time and volume. Comparing (8) and (12) we find

$$P_{\text{in}}(t) \triangleq d\bar{S}/dt - (\Gamma g(n) - \kappa)\bar{S}. \quad (13)$$

In the present theory  $\bar{S}(t)$  is calculated self-consistently from the coupled equations (7, 9, 10). Therefore, the full nonlinear feedback of the electrons upon the signal wave, and vice versa, is included, incorporating the effects of dynamic gain and of signal transit time delays. These feedback effects are ignored if  $P_{\text{in}}(t)$  is used as a fixed given input function [2, 3, 8]. The latter amounts to assuming that the rhs of (13) is, up to a proportionality constant, equal to  $|E_{\text{in}}(t)|^2$ .

### 3. Numerical Results and Comparison to Experiment

We shall now apply the theory to the experimental setup of Sect. 1. In the following numerical simulations the injection current is modelled by an asymmetric Gaussian

$$J(t) = \begin{cases} J_0 \exp\{-[(t-t_0)/t_r]^2\} & \text{for } t < t_0 \\ J_0 \exp\{-[(t-t_0)/t_f]^2\} & \text{for } t \geq t_0 \end{cases} \quad (14)$$

and the optical input signal is approximated by a simple Gaussian

$$E_{\text{in}}(t) = E_0 \exp\{-[(t-t_0+\tau_d)/t_s]^2\} \quad (15)$$

Table 1. Numerical parameters used in the simulations

$t_r = 72$ ps	$B = 1.6 \times 10^{-10}$ cm <sup>3</sup> s <sup>-1</sup>	$\alpha = 0.15$ ps <sup>-1</sup>
$t_f = 145$ ps	$g_0 = 4 \times 10^{-6}$ cm <sup>3</sup> s <sup>-1</sup>	$R_1 = R_2 = 0.33$
$t_0 = 500$ ps	$n_0 = 1.25 \times 10^{18}$ cm <sup>-3</sup>	$L = 300$ μm
$t_s = 50$ ps	$\Gamma = 0.2$	$n_g = 4$
	$\beta = 10^{-3}$	$k = 2\pi n_g/\lambda_0$
	$\kappa = 1$ ps <sup>-1</sup>	$\lambda_0 = 0.8$ μm

The resulting cw threshold carrier density is  $n_t = 2.5 \times 10^{18}$  cm<sup>-3</sup>.  $\bar{S}(t)$  has been varied in the simulations in discrete time steps of 0.5 ps

where  $\tau_d$  measures the time delay between the maxima of the electrical and optical input pulse. The numerical parameters are given in Table 1; they lead to a FWHM of  $|E_{\text{in}}(t)|^2$  of 60 ps. These input functions closely approximate the experimentally used pulses. The spontaneous recombination rate and the modal gain are modelled by

$$R_{sp} = Bn^2, \quad (16)$$

$$g = g_0(n - n_0) \quad (17)$$

with material constants  $B$ ,  $g_0$ ,  $n_0$ . All material parameters used in the calculations are summarized in Table 1. In view of the large uncertainties in these parameters, we have not attempted to reach a best fit, but have used typical parameter values from the literature. In particular, the total loss coefficient  $\kappa$  [13] of the cavity modes, the absorption coefficient  $\alpha$  [5] of the signal mode, and the reflectivity  $R$  [4] have been chosen as independent quantities, cf. the critical discussion about the different approximations involved in the rate equations versus Fabry-Perot approach [17, 19, 20]. It has been checked by varying some of these parameters that the qualitative features of the numerical solutions are widely insensitive to the choice of the particular values. Here our main concern is to understand the physical mechanism.

Figure 6 shows the results of the simulations for an injection current pulse (14) with  $J_0/J_t = 10$  where  $J_t$  is the cw threshold, and for optical input signals (15) of peak values  $E_0$  decreasing from (a) to (c). For the injection current shape chosen,  $J_0/J_t = 10$  corresponds to excitation conditions below the dynamic effective threshold, i.e., no laser emission (relaxation oscillation)  $N(t)$  is obtained for  $E_{\text{in}} = 0$ . The total optical output intensity<sup>2</sup>  $\int (N + |E_{\text{out}}|^2) dt$  integrated over 1 ns is plotted versus the time delay  $\tau_d$ . Under these injection conditions,  $\int N dt$  is negligible. Amplification of the input signal occurs when it falls within a time window *after* the peak injection current. It can be seen that the maximum of the curves decreases and the FWHM

<sup>2</sup> For the field units chosen,  $N$  and  $|E_{\text{out}}|^2$  both have the dimension of a photon density rather than intensity

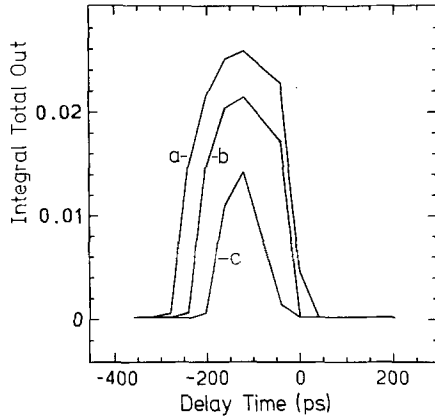


Fig. 6. Integrated total optical output intensity  $\int (N + |E_{\text{out}}|^2) dt$  in arbitrary units versus time delay  $\tau_d$  in ps between the electrical and the optical pulse under current injection conditions below dynamical threshold ( $J_0/J_t = 10$ ) for a sequence of decreasing peak optical input signals. *a*  $E_0 = 4 \times 10^{-8}$ , *b*  $E_0 = 2 \times 10^{-9}$ , *c*  $E_0 = 10^{-10}$ . The unit of  $E_0$  is  $n_t^{1/2}$ ; the numerical parameters are given in Table 1

decreases from 220 to 100 ps with decreasing input intensities, in very good agreement with the experimental results (Fig. 3).

This behaviour can be understood by considering the electron density  $n$  and the single-pass gain  $G_s$  as a function of time. Without an optical input signal the electron density rises to a maximum which occurs 200 ps after the peak of the injection current pulse, and then slowly decreases via spontaneous recombination. The maximum  $n$  is still below the threshold value  $n_t = n_0 + \kappa/(\Gamma g_0)$  such that no self-generated laser action (relaxation oscillation) occurs, see (8). However, amplification of an incident signal is possible, since the single-pass gain  $G_s(t)$  is greater than unity as long as  $n > n_0 + \alpha/(\Gamma g_0)$  with  $\alpha < \kappa$ . The condition  $RG_s(t) > 1$  defines a gain window in the *time regime*. A measurable output signal is produced if the input signal experiences a sufficient number of roundtrips during this gain window. The largest net amplification is obtained if the input signal is injected somewhat before the maximum of  $n$  (and thus of  $G_s$ ) occurs, in order to allow for the finite build-up time of the signal wave inside the cavity. This explains the position of the peak integral output in Fig. 6 at about 100 ps after the peak injection current ( $\tau_d \approx -100$  ps). If the signal is injected too early or too late the signal wave cannot build up sufficiently fast inside the cavity to produce an output. For smaller initial signal input intensities, more round trips of the signal are required to fall within the gain window in order to reach the same output signal intensity. The width of the effective optical gate in the *delay time regime* is thus decreased. The narrowing of the optical gate with decreasing input intensity in Fig. 6a–c, and Fig. 3a–c is thus understood.

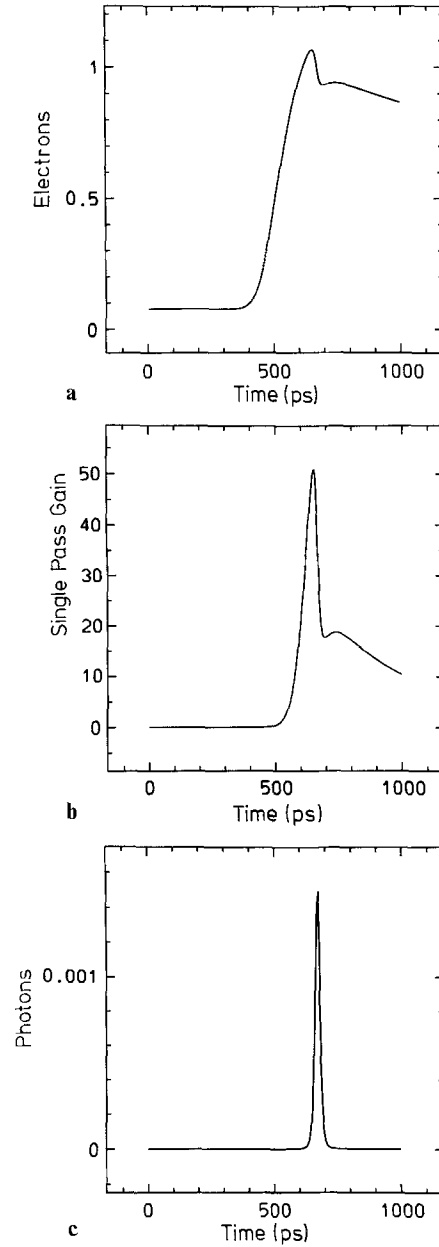


Fig. 7. (a) Electron density  $n/n_t$ , (b) single-pass gain  $G_s$ , (c) photon density  $N/n_t$  versus time in ps for  $J_0/J_t = 15$  and  $E_0 = 0$ , and the parameters of Table 1

The photon densities corresponding to the input signal of Fig. 6 are many orders of magnitude smaller than the photon densities of the relaxation oscillations emitted above threshold. Under these conditions the effect of the signal wave upon the electron density, i.e., the gain depletion by the enhanced stimulated emission of the amplified signal, is slight. At larger input intensities, this effect drastically reduces the falling shoulder of the single-pass gain [12].

Next, we consider current injection conditions slightly above the dynamic effective threshold, such that just a single relaxation oscillation is emitted for

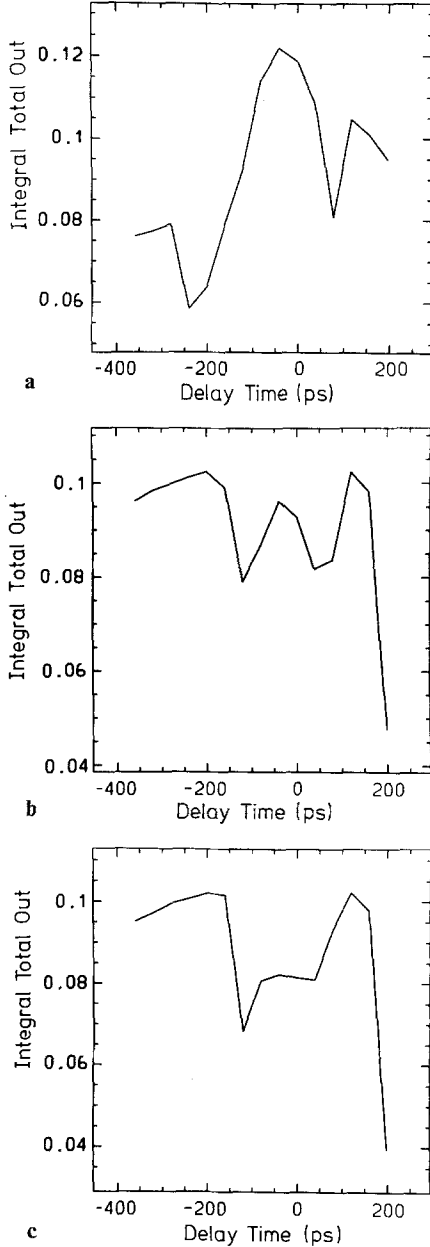


Fig. 8a–c. Integrated total optical output intensity  $\int (N + |E_{\text{out}}|^2) dt$  in arbitrary units versus time delay  $\tau_d$  in ps under current injection conditions above dynamical threshold ( $J_0/J_t = 15$ ) for a sequence of decreasing peak optical input signals: (a)  $E_0 = 10^{-2}$ , (b)  $E_0 = 5 \times 10^{-6}$ , (c)  $E_0 = 10^{-7}$ . The numerical parameters are given in Table 1

$E_{\text{in}} = 0$  (Fig. 7). The electron density reaches a maximum  $n > n_t$ , and the single-pass gain  $G_s(t)$  is given by a very narrow peak superimposed to a much lower and broader background peaking at later times. In Fig. 8, the total optical output intensity  $\int N dt + \int |E_{\text{out}}|^2 dt$  integrated over 1 ns is plotted versus the time delay  $\tau_d$  for three different input signal intensities. In addition to the main peak, a smaller peak appears to its right (Fig. 8a) corresponding to input signals injected ear-

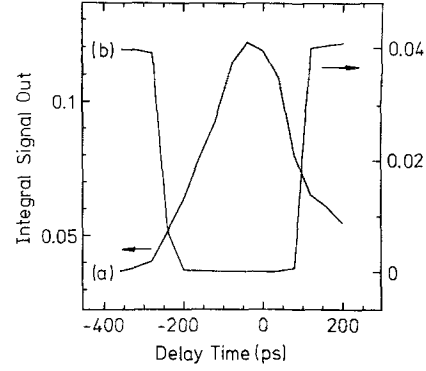


Fig. 9. a Integrated amplified signal output  $\int |E_{\text{out}}|^2 dt$  (left scale). b Integrated amplified spontaneous emission  $\int N dt$  (right scale) versus time delay  $\tau_d$  in ps for  $J_0/J_t = 15$  and  $E_0 = 10^{-2}$  and the parameters of Table 1

lier. With decreasing input signal intensity the central peak becomes lower (Fig. 8b) and disappears (Fig. 8c), while the rhs peak remains. This behaviour reproduces our experimental findings quite well (Fig. 4). It can be understood by considering the contributions of the amplified signal  $\int |E_{\text{out}}|^2 dt$  and of the amplified spontaneous emission  $\int N dt$  separately (Fig. 9). The central peak in Fig. 8a corresponds to the peak of the amplified signal (Fig. 9a), which occurs for input signals impinging *after* the maximum of the injection current pulse. This peak decreases with decreasing input signal intensities. The mechanism is similar to that which is operative below the dynamic effective threshold (Fig. 6). The additional rhs peak in Fig. 8a which occurs for input signals impinging *before* the maximum of the injection current pulse is due to the competition of the amplified signal and amplified spontaneous emission. The dip between these two peaks is due to the sharp quenching of the amplified spontaneous emission for delay times  $\tau_d < 100$  ps (Fig. 9b). This quenching is the result of the dynamic gain depletion by the amplified signal as discussed previously [12]. The pronounced step-like reduction of the amplified spontaneous emission is retained at lower input signal intensities. This explains the weak dependence of the rhs peak in Fig. 8 upon the input signal intensity. The gain depletion is illustrated in Fig. 10a–c by plots of  $n(t)$ ,  $G_s(t)$ , and  $|E_{\text{out}}(t)|^2$  for the same parameters as in Fig. 7, but with  $E_0 = 10^{-2}$  and  $\tau_d = 0$ . The amplified signal wave reduces the carrier density by strongly enhanced stimulated emission such that the threshold density  $n_t$  is not reached (Fig. 10a) and the relaxation oscillations of  $N(t)$  are heavily quenched. The single-pass gain  $G_s$  (Fig. 10b), however, is still high enough to allow for signal amplification (Fig. 10c).

Figure 10d shows the electron density for a value of the delay time  $\tau_d$  corresponding to the rhs peak in Fig. 8a. Since the input signal occurs earlier than in

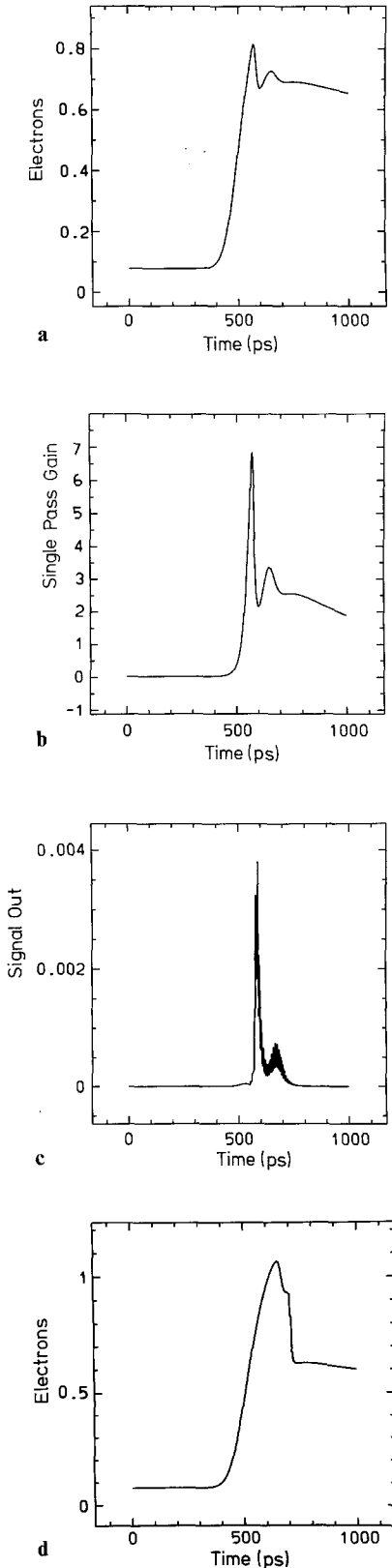


Fig. 10. (a) Electron density  $n/n_t$ , (b) single-pass gain  $G_s$ , (c) Photon density  $|E_{out}|^2/n_t$  of the amplified output signal versus time in ps for  $J_0/J_t = 15$ ,  $E_0 = 10^{-2}$ ,  $\tau_d = 0$ , and the parameters of Table 1. (d) Same as (a), but for  $\tau_d = 120$  ps

Fig. 10a, the initial gain is smaller, and the signal wave cannot build up fast enough to inhibit the rise of the electron density and of the single-pass gain. Therefore,  $n$  exceeds the threshold density  $n_t$ , and both the amplified spontaneous emission (relaxation oscillation) and the amplified signal wave contribute to the output signal (Fig. 9).

The additional shoulder for large negative delay times in Fig. 8 is probably caused by the slight overestimation of the signal amplification in the present theory, an effect which accumulates during the slow decay of the electron concentration  $n(t)$  (Fig. 7a). This allows for amplification of the input signal even if the input signal impinges very late after the injection current pulse.

#### 4. Conclusion

A detailed experimental and theoretical investigation of the dynamical optical boxcar effect which was recently discovered for gain switched semiconductor lasers is reported. Amplification by the gate laser driven slightly below and above dynamical threshold is investigated. The integral optical output intensity as a function of the delay time  $\tau_d$  is studied under different operation conditions of the laser amplifier, viz. electrical injection currents, and for different optical input intensities. The physical mechanism which leads to the observed optical gate in the delay time regime is explained in terms of a recently developed theory of coherent time-dependent optical amplification which includes the nonlinear dynamics of the semiconductor laser. The narrowest gate width is observed if the laser amplifier is driven slightly above its dynamical threshold, and if the optical input is attenuated sufficiently. This is shown by the simulations to be caused by the narrow single-pass gain maximum associated with the first relaxation oscillation of the gate laser. This effect can be used to detect optical pulses with a time resolution better than 10 ps [11], which is similar to that of synchroscan streak cameras. A wide range of applications is evident for such sensitive optical gates. This is another example for the great importance of nonlinear dynamic behaviour in semiconductors [21].

#### References

1. J.C. Simon: *J. Opt. Commun.* **4**, 51 (1983)
2. T. Mukai, Y. Yamamoto, T. Kimura: In *Semiconductors and Semimetals*, ed. by W.T. Tsang (Academic, Orlando 1985) Vol. 22, Part E, pp. 265–319
3. T. Mukai, Y. Yamamoto, T. Kimura: *Rev. Electr. Commun. Labs.* **31**, 340 (1983)
4. M.J. Adams, J.V. Collins, I.D. Henning: *IEE Proc.* **132**, 58 (1985)
5. D. Marcuse: *IEEE J. QE-19*, 63 (1983)
6. J. Buus, B. Plastow: *IEEE J. QE-21*, 614 (1985)

7. J. Hegarty, K.A. Jackson: Appl. Phys. Lett. **45**, 1314 (1984)
8. M. Ikeda: IEEE J. QE-**19**, 157 (1983)
9. B.C. Johnson, A. Mooradian: Appl. Phys. Lett. **49**, 1135 (1986)
10. W. Lenth: Opt. Lett. **9**, 396 (1984)
11. K. Ketterer, E.H. Böttcher, D. Bimberg: Appl. Phys. Lett. **50**, 1471 (1987)
12. E. Schöll: IEEE J. QE-**24** (Feb. 1988)
13. D. Bimberg, K. Ketterer, E.H. Böttcher, E. Schöll: Int'l. J. Electron. **60**, 23 (1986)
14. D.E. Ackley, G. Hom: Appl. Phys. Lett. **42**, 653 (1983)
15. E.H. Böttcher, K. Ketterer, D. Bimberg: J. Appl. Phys. (Jan. 1988)
16. E. Schöll, D. Bimberg, H. Schumacher, P.T. Landsberg: IEEE J. QE-**20**, 394 (1984)
17. K.Y. Lau, A. Yariv: In *Semiconductors and Semimetals*, ed. by W.T. Tsang (Academic, Orlando 1985) Vol. 22, Part B, pp. 70–152
18. H. Haug: Phys. Rev. **184**, 338 (1969)
19. D.T. Cassidy: Appl. Opt. **22**, 3321 (1983)
20. G.H.B. Thompson: *Physics of Semiconductor Laser Devices* (Wiley, London 1980)
21. E. Schöll: *Nonequilibrium Phase Transitions in Semiconductors*, Springer Series in Synergetics, Vol. **35** (Springer, Berlin, Heidelberg 1987)